Songklanakarin J. Sci. Technol.
32 (5), 481-488, Sep. - Oct. 2010

Songklanakarin Journal of Science and Technology
http://www.sjst.psu.ac.th

Original Article

Iterated Viterbi detection methods for a 2-D bit patterned mediastorage

Lin M. M. Myint[1]*, Pornchai Supnithi[2] and Prinya Tantaswadi[1]

[1] *School of Technology,*
Shinawatra University, Sam Khok, Pathum Thani 12160, Thailand.

[2] *Faculty of Engineering and College of Data Storage Technology and Applications,*
King Mongkut's Institute of Technology Lat Krabang, Bangkok, 10520, Thailand.

Received 26 March 2010; Accepted 9 August 2010

Abstract

In this paper, we studied the performance of the iterated Viterbi detection methods using the multi-track multi-head processing for a bit patterned media (BPM) channel with a two-dimensional interference consisting of inter-symbol interference (ISI) and inter-track interference (ITI). In each method, three Viterbi detectors are employed to process the three readback signals. In their trellises, the number of states is designed based on the ISI only. After the first iteration, the estimated output sequences are exchanged between the adjacent detectors as the ITI estimations and then used in the metric calculation of next iteration. When compared with other methods, the simulation results show that the proposed methods achieve significant gains. We also investigated the performance of the proposed methods for the BPM channel with different media noise levels. Finally, the computational complexity of all detectors is compared.

Keywords: inter-track interference, inter-symbol interference, bit patterned media storage, multi-track detection, Viterbi algorithm, media noise

1. Introduction

For conventional magnetic media, the increment of the recording density is projected to saturate in the near future. The recording density in the magnetic media is increased by reducing the recorded bit size on the media. In theory, the signal-to-noise ratio (SNR) depends on the number of magnetic grains per recorded bit, hence a sufficient amount of grains per bit needs to maintain in order to achieve an acceptable SNR while increasing the recording density. The reduction in grain size, however, weakens the thermal stability of the magnetic particles, which leads to a randomization of the magnetization of the record bits. This phenomenon is known as the super-paramagnetic effect (Nutter *et al.*, 2005; Nabavi and Kumar, 2007; Karakulak *et al.*, 2008a). At present, a number of viable advanced magnetic recording technologies are available: bit patterned media recording (BPMR), heat assisted magnetic recording (HAMR), microwave assisted magnetic recording (MAMR), and recently, two-dimensional magnetic recording (TDMR) are proposed to increase the recording density to the next goal of 10 terabits/in^2 beyond the super-paramagnetic effect limit (Shiroishi *et al.*, 2009).

In bit patterned media (BPM) technology, each data bit is recorded in a fabricated single-domain magnetic island, which is composed only of a single magnetic grain. Each magnetic island is strongly coupled and the grain can maintain the size. As a result, the grain islands in the BPM media are thermally stable. Moreover, non-magnetic regions between islands can eliminate the transition noise, which is a prominent noise in the conventional magnetic media (Nutter *et al.*, 2005; Shroishi *et al.*, 2009). Thus, the readback signal from the BPM media contains less noise, which can improve the SNR in the data recovery system. However, due to the imperfection in the fabrication process, the size and location

* Corresponding author.
Email address: lin@siu.ac.th

of each bit island may vary from the expected size and location; the size and location fluctuation in the BPM system may generate the media noise in the readback signal (Nabavi *et al.*, 2008; Nabavi *et al.*, 2009). To study the performance of the readback channel, the media noise is considered as the prominent noise in the BPM channel.

Besides the media noise, the readback signal from the BPM system is corrupted by a two-dimensional (2-D) interference: inter-symbol interference (ISI) and inter-track interference (ITI) because the separations between adjacent islands both along-track and cross-track directions require to be reduced in order to acquire the high recording density. This 2-D interference degrades the bit error rate (BER) performance in the data recovery system and is one of the main challenges in the BPM and other high density storage technologies. For a 1-D interference channel, a maximum-likelihood sequence detector (MLSD), in particular, a Viterbi detector, in which the trellis is designed based on the ISI, is normally employed for the data recovery. On the other hand, it does not perform well in the 2-D interference channels. Therefore, a 2-D Viterbi detector, which incorporates both the ISI and ITI effects in its trellis, is required for the 2-D interference channel. Nevertheless the 2-D Viterbi detector is infeasible to be implemented in hardware because of its excessive complexity. The computational complexity in the 2-D Viterbi detector grows exponentially with the number of ITI and ISI taps in the channel.

Recently, a number of Viterbi-based detectors for the 2-D interference channel (Burkhardt, 1989; Heanue *et al*., 1996; Nabavi and Kumar, 2007; Nabavi *et al*., 2007; Keskinoz, 2008) have been proposed. In Burkhardt (1989), an optimal 2-D Viterbi detector, in which the trellis is designed by considering each column of bits as a symbol, is devised for the 2-D channel but the complexity is still too high to be implemented, even for a moderate number of ISI and ITI. In order to reduce the complexity in the 2-D detector, a modified Viterbi algorithm for the 2-D BPM channels (Nabavi *et al*., 2007) is proposed by incorporating the most influential ITI effects in its trellis. Alternatively, some researchers introduced a 2-D generalized partial response equalizer, which eliminates the ITI effects and keeps only the controlled ISI, followed by a conventional 1-D Viterbi detector (Nabavi and Kumar, 2007; Keskinoz, 2008). In optical storage, the Viterbi detection with decision feedback (Heanue *et al.*, 1996) provides the performance improvement of the 2-D page access memory optical channel. In this method, the detector operates on a row-by-row basis for the 512x512 rectangular data array. Moreover, a multi-track Viterbi algorithm (MVA) based on the stripe-wise trellis approach is proposed in Hekstra *et al*. (2007) for the 2-D optical channel by exploiting the multi-track processing in optical storage.

In this study, we propose the iterated Viterbi detection methods for the 2-D BPM channel by exploiting the multi-track multi-head processing. For a 3x3 channel matrix of BPM, we assume that the three readback signals are obtained, then each of which is processed by one of the three Viterbi detectors. Each detector employs a simple trellis, which is constructed based on the ISI effect only, and the ITI effect is however involved in the branch metric calculation. After the first iteration, the estimated hard output sequences are exchanged between the adjacent detectors as the ITI estimations and then applied in the metric calculation of the next iteration. Two variants of the proposed detection methods are investigated.

The remainder of this paper is organized as follows. In Section 2, we describe the BPM readback channel model. Section 3 presents the details of the proposed iterated Viterbi detection methods. In Section 4, we provide the simulation results and discussions. Finally, conclusions are given in Section 5.

2. BPM Readback Channel Model

In a BPM system, the readback signal from a bit island is corrupted by the interference from the adjacent bit islands as well as from the bit islands on the adjacent tracks and an accurate readback pulse response of an isolated bit island can be generated by using the extended reciprocity integral from Nutter *et al.* (2005) over a 3-D space. However, it can also be approximately synthesized by a mathematical equation such as a Lorentzian equation or a Gaussian equation (Nabvi *et al*., 2009). The shape of the readback pulse of the isolated bit varies depending on the media with soft underlayer (SUL) or without SUL. The pulse response for the media with SUL has a unipulse shape. But, in the case without SUL, the triplet pulse shape arises because the pulse is the summation of the two opposite polarity charge pulses from the upper and bottom surfaces. The pulse produced by the bottom surface charge has a smaller amplitude and broader width than the pulse from the upper surface charge (Nutter *et al.*, 2005; Nabavi and Kumar, 2007).

In this work, we studied the perpendicular BPM channel in the discrete-time domain. The readback channel is modelled as a 2-D interference channel with both ISI and ITI. The readback signal from the k^{th} bit island along the l^{th} track, $r_{k,l}$, can be expressed as

$$r_{k,l} = \sum_n \sum_m h_{n,m} x_{k-n,l-m} + n_{k,l} \qquad (1)$$

where $x_{k-n,l-m}$ are the recorded bits on the islands along the current track and the adjacent tracks, $h_{n,m}$'s are the 2-D channel response coefficients, and $n_{k,l}$ is assumed to be the additive white Gaussian noise (AWGN). Considering a 3x3 bit islands of a BPM as illustrated in Figure 1, the read head reads from a bit island under it whereas it also suffers the interference from two adjacent islands on the same track and two neighbour islands together with four cornered islands on two adjacent track. Based on that, a discrete-time readback channel model is represented by a symmetric 3x3 matrix in (Nabavi *et al.*, 2007; Karakulak *et al.*, 2008a) as

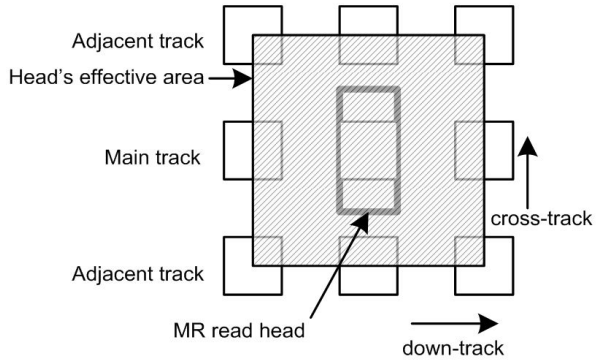

Figure 1. Read head affective area over the 3x3 bit islands in the BPM.

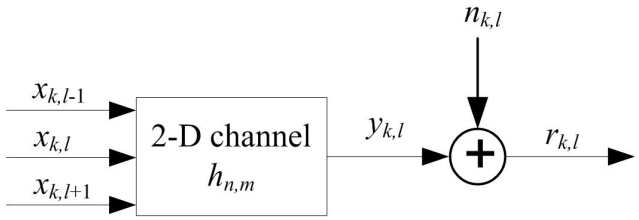

Figure 2. Channel model of the BPM system.

$$\mathbf{H} = \begin{pmatrix} h_{-1,-1} & h_{0,-1} & h_{1,-1} \\ h_{-1,0} & h_{0,0} & h_{1,0} \\ h_{-1,1} & h_{0,1} & h_{1,1} \end{pmatrix} = \begin{pmatrix} \alpha & a & \alpha \\ \beta & 1 & \beta \\ \alpha & a & \alpha \end{pmatrix} \tag{2}$$

where β is the ISI coefficient on the same track, a is the ITI coefficient due to the islands immediately above and below, and α is the ITI coefficient due to the cornered islands as shown in Figure 1. With the channel coefficients in Equation 2, the readback signal in Equation 1 can be expanded as

$$\begin{aligned} r_{k,l} &= x_{k,l} + \beta(x_{k-1,l} + x_{k+1,l}) + a(x_{k,l-1} + x_{k,l+1}) \\ &\quad + \alpha(x_{k-1,l-1} + x_{k-1,l+1} + x_{k+1,l-1} + x_{k+1,l+1}) + n_{k,l}. \\ &= y_{k,l} + n_{k,l} \end{aligned} \tag{3}$$

where $y_{k,l}$ is the noiseless channel output as shown in Figure 2. In Equation 3, the first and second terms are related to the current bit and the ISI effects due the two adjacent bits on the current l^{th} track and the third and fourth terms are the ITI effects due to the two adjacent tracks (l-1) and (l+1).

Thus, in order to analyse the readback channel performance of the BPM, the accurate readback pulse response is generated by using the extension of reciprocity integral over 3-D space in (Nutter *et al.*, 2005). However, in order to avoid the complex reciprocity integral, the readback pulse response of an isolated island for both media can be approximately synthesized by a Gaussian pulse response (Nabavi *et al.*, 2008). The channel response coefficients are obtained by sampling the 2-D pulse response of the isolated island at the integer multiples of the bit period and track pitch (Nabavi and Kumar, 2007). The 2D Gaussian pulse response for the BPM media with media noise from Nabavi *et al.* (2008) is

$$P(x,z) = (A + \Delta_A)\exp\left\{-\frac{1}{2}\left[\left(\frac{x+\Delta_x}{c(PW_x + \Delta_{PWx})}\right)^2 + \left(\frac{z+\Delta_z}{c(PW_z + \Delta_{PWz})}\right)^2\right]\right\} \tag{4}$$

where A is the amplitude, x and z are in along-track direction and in cross-track direction, and PW_x and PW_z are the $PW50$s of the pulse response. For the media noise in Equation 4, Δ_A is the amplitude fluctuation, Δ_x and Δ_y are the location fluctuation, and Δ_{PWx} and Δ_{PWz} are the PW50 fluctuation in along-track and cross-track direction. The location and size fluctuation in the channel can be modelled by a Gaussian process. The standard deviation of the fluctuation can be defined as the percentage of the bit period. The channel response coefficients in the matrix in Equation 2 can be calculated by

$$h_{m,n} = P(mT_x,\ nT_z), \qquad m,n \in -1,0,1 \tag{5}$$

where T_x is the bit period and T_z is the track pitch.

3. Iterated Viterbi Detection

3.1 Iterated Viterbi detection method I

In this paper, we propose an iterated Viterbi detection technique for the 2-D interference BPM channel by exploiting the multi-track multi-head processing. The proposed model is illustrated in Figure 3. In the model, we assume that the readback signals from the three adjacent tracks are detected simultaneously by a multi-head array and then the read signals are sent to the inputs of the three Viterbi detectors separately to recover the recorded input bits. The trellis of each detector is simply designed with the ISI effects only as shown in Figure 4(a).

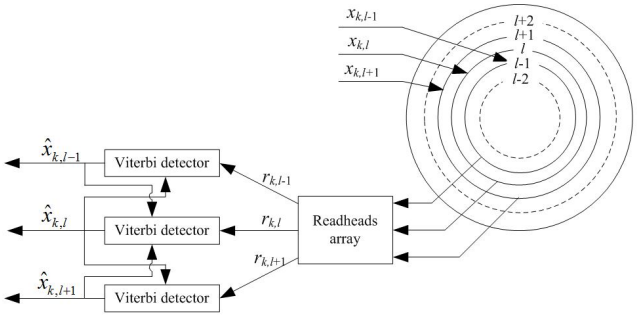

Figure 3. Proposed model for the BPM recording system with multi-track processing.

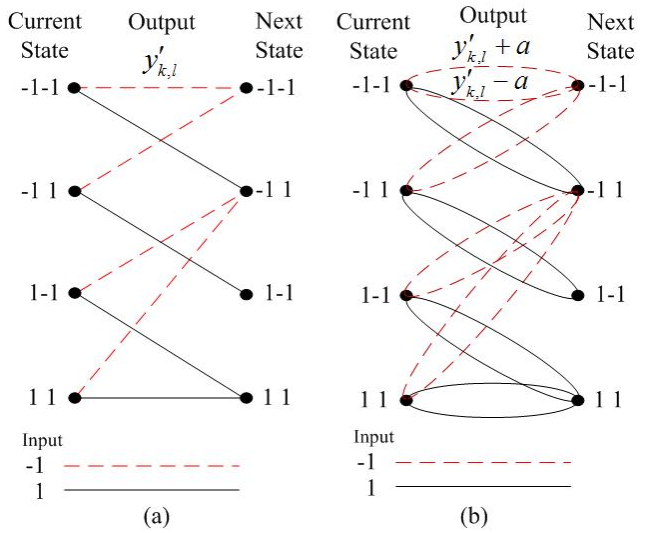

Figure 4. Trellis diagrams of the Viterbi detectors (a) for the proposed method I and (b) for the outer detectors in the proposed method II.

According to Equation 2 and 3, the readback signal is affected by two ISI bits, thus having four states with two outgoing branches from each state in the trellis. In the detection algorithm, the branch metric for the state transition is computed by incorporating the effects of ITI in order to determine the survivor path at each state. In the Viterbi algorithm of the detector for the track l, the branch metric $\lambda_{k,l}^{s'\to s}$ for each state transition from the current state s to the next state s at time k (Vucetic and Yuan, 2000) is computed as

$$\lambda_{k,l}^{s'\to s} = \left(r_{k,l} - y_{k,l}\right)^2 \tag{6}$$

where $r_{k,l}$ is the received signal at the input of the detector and $y_{k,l}$ is the ideal noiseless channel output which can be expressed from Equation 3 as

$$y_{k,l} = y'_{k,l} + a(\hat{x}_{k,l-1} + \hat{x}_{k,l+1}) + \alpha(\hat{x}_{k-1,l-1} + \hat{x}_{k-1,l+1} + \hat{x}_{k+1,l-1} + \hat{x}_{k+1,l+1}). \tag{7}$$

In Equation 7, the first term $y'_{k,l}$ corresponds to the branch output from the trellis from Figure 4(a). The branch output $y'_{k,l}$ is calculated with the current input bit and the ISI bits as,

$$y'_{k,l} = x_{k,l} + \beta(x_{k-1,l} + x_{k+1,l}). \tag{8}$$

The remaining terms are the ITI effects due to the upper and lower tracks and they are required as the extrinsic information from other adjacent detectors. With the knowledge of the ITI coefficients a and α, these two terms can be computed using the estimated bit sequences ($\hat{x}_{k-1,l-1}$, $\hat{x}_{k,l-1}$, $\hat{x}_{k+1,l-1}$) from the upper $(l\text{-}1)^{\text{th}}$ track and ($\hat{x}_{k-1,l+1}$, $\hat{x}_{k,l+1}$, $\hat{x}_{k+1,l+1}$) from the lower $(l\text{+}1)^{\text{th}}$ track as the ITI estimation from the iterative process.

At the first iteration, each of these Viterbi detectors processes the readback signal with the information from the trellis only since no extrinsic information is available. Thus, the ideal noiseless channel output in Equation 7 is equal to the branch output $y'_{k,l}$ from the trellis. After the first iteration, each detector generates the estimated input bit sequence from its respective track at its output. Even though these estimated bit sequences have low reliability, they can be exchanged among the detectors to be used as the ITI estimations for the next iteration. With the estimated sequences from the tracks (l-1) and (l+1), the middle detector can compute the noiseless channel output $y_{k,l}$ for the track (l) as in Equation 7. However, the upper and lower detectors receive only one-side ITI estimation from the middle detector of the track (l) because the ITI estimation from the track (l-2) and (l+2) are not available in the proposed system as shown in Figure 3. Therefore, the noiseless channel outputs $y_{k,l-1}$ and $y_{k,l+1}$ for the tracks (l-1) and (l+1) in these detectors are generated with one-side ITI estimation as

$$y_{k,l-1} = y'_{k,l-1} + a(\hat{x}_{k,l}) + \alpha(\hat{x}_{k-1,l} + \hat{x}_{k+1,l}), \tag{9}$$

and

$$y_{k,l+1} = y'_{k,l+1} + a(\hat{x}_{k,l}) + \alpha(\hat{x}_{k-1,l} + \hat{x}_{k+1,l}). \tag{10}$$

In Equation 9 and 10, $y'_{k,l-1}$ and $y'_{k,l+1}$ are the branch outputs of the trellis similar to $y'_{k,l}$ in Equation 7 and, ($\hat{x}_{k-1,l}$, $\hat{x}_{k,l}$, $\hat{x}_{k+1,l}$) are the ITI estimations from the middle track (l). Using these updated noiseless channel outputs, the detectors at the new iteration generate the branch metric for each state transition with more reliable values than those at the previous iteration.

In the proposed method, the outer detectors for the tracks (l-1) and (l+1) receive one-side ITI estimation only; as a result, the proposed method is not optimal. Another disadvantage of this method is an error propagation problem, but a robust error correction code like the low-density parity-check (LDPC) code can be applied to reduce the errors from the estimated bits.

3.2 Iterative Viterbi detection method II

To address the partial ITI in the method I, the trellis for the outer detectors for the tracks (l-1) and (l+1) are modified similar to Nabavi *et al.*(2007) but the middle detector still uses the trellis from Figure 4(a). In the modified trellis, the number of the states still depends on the ISI effects, while the number of parallel branches between connected states is expanded based on the unavailable ITI effects from the iterative process. The noiseless channel output equation for the track (l-1) from Equation 9 is rearranged by incorporating all ITI effects from the two adjacent tracks (l) and (l-2) as

$$y_{k,l-1} = y'_{k,l-1} + a\hat{x}_{k,l-2} + \alpha\left(\hat{x}_{k-1,l-2} + \hat{x}_{k+1,l-2}\right) + a\hat{x}_{k,l} + \alpha\left(\hat{x}_{k-1,l} + \hat{x}_{k+1,l}\right). \tag{11}$$

where the first term, the branch output from the trellis, is determined by the state transitions and the last two terms related to the ITI effects from the track l can be obtained from the ITI estimation from the middle detector. The second and third terms are the ITI effects due to the track (l-2), which are not available from the system, and these information are required to estimate within the trellis. The empirical results show that the ITI effects from the cornered islands are not significant due to the small value of coefficient α in the channel matrix from Equation 2 and thus those ITI effects are ignored in this method. Taking the knowledge of the value of $x_{k,l-2}$ be {-1,1}, the noiseless channel output from Equation 11 can have two possible values, i.e.,

$$y_{k,l-1} = \begin{cases} y'_{k,l-1} - a + a\hat{x}_{k,l} + \alpha\left(\hat{x}_{k-1,l} + \hat{x}_{k+1,l}\right) \\ y'_{k,l-1} + a + a\hat{x}_{k,l} + \alpha\left(\hat{x}_{k-1,l} + \hat{x}_{k+1,l}\right) \end{cases} \cdot \quad (12)$$

In Equation 12, the two equations correspond to the case when $x_{k,l-2}$ is -1 and $x_{k,l-2}$ is +1. Finally, the trellis is redesigned by expanding two parallel branches, with branch outputs ($y'_{k,l-1}$ - a) and ($y'_{k,l\,l-1}$ + a), between each pair of connected states as shown in Figure 4(b). Similarly, the trellis of the detector for the track (l+1) is modified to achieve the two possible noiseless channel outputs,

$$y_{k,l+1} = \begin{cases} y'_{k,l+1} - a + a\hat{x}_{k,l} + \alpha\left(\hat{x}_{k-1,l} + \hat{x}_{k+1,l}\right) \\ y'_{k,l+1} + a + a\hat{x}_{k,l} + \alpha\left(\hat{x}_{k-1,l} + \hat{x}_{k+1,l}\right) \end{cases} \cdot \quad (13)$$

4. Simulation Results and Discussions

In the simulation model, we assume that the recording channel employs the multi-head multi-track processing as shown in Figure 3. In this study, we consider the simulation model in the discrete-time domain only. We assume that the channel is known and the trellis for all detectors is constructed based on the channel coefficients. For all detectors, we do not consider an equalizer for PR target or GPR target, hence. Note that in the simulation, we also consider the contributions of $x_{k,l-2}$ and $x_{k,l+2}$ as the ITI effects on the read sequence $r_{k,l-1}$ and $r_{k,l+1}$, respectively.

We consider the 3x3 channel response matrices for 1 Tb/in^2 with a square island of size 12.5 nm and the bit period T_x and the track pitch T_z of 21 nm (from Nabavi *et al.*, 2007; Karakulak *et al.*, 2008b), i.e.,

$$\mathbf{H}_A = \begin{pmatrix} -0.023 & 0.264 & -0.023 \\ -0.087 & 1 & -0.087 \\ -0.023 & 0.264 & -0.023 \end{pmatrix}, \quad (14)$$

and

$$\mathbf{H}_B = \begin{pmatrix} 0.0347 & 0.2297 & 0.0347 \\ 0.1277 & 1 & 0.1277 \\ 0.0347 & 0.2297 & 0.0347 \end{pmatrix}. \quad (15)$$

The matrix $\mathbf{H}_A$ is for the BPM channel without SUL and the coefficients of the ISI and the cornered ITI have the negative values because of the triplet shape of the readback pulse. The matrix $\mathbf{H}_B$ is for the case with SUL. The signal-to-noise ratio (SNR) is defined as 20log(Vp/σ), where Vp is the peak value of the readback signal, and σ is the standard deviation of AWGN. In the simulation, we also consider the BPM media with the two guard bands (no recorded information) for the two outer ITI tracks (l-2) and (l+2) as the baseline. Therefore, the readback signal from the tracks (l-1) and (l+1) have no ITI effects from those outer tracks and there is no more partial ITI estimation problem in the proposed method I at the expense of the recording density.

Firstly, we studied the performance of the proposed iterated Viterbi detection method I with various numbers of iterations for the BPM channel $\mathbf{H}_A$. In Figure 5, the results show the performance gain of the proposed method I over the number of iterations. At the first iteration, the proposed iterated Viterbi detection method processes the readback signal without any extrinsic ITI information; hence, their performances are similar to the conventional Viterbi detectors. However, from the 2nd iteration onward, the proposed method achieves the gain due to the ITI estimation from the previous iteration. After the 3rd iteration, there is no more significant performance gain.

In Figure 6, the performance of the iterated Viterbi detection method I (IterVit I) and II (IterVit II) for the BPM channel $\mathbf{H}_A$ are compared with that of the method I with guard bands. Both methods without the guard bands lose about 2-dB to the method I with the guard bands because the iterated Viterbi detection with guard bands has no partial ITI estimation problem or is without any ambiguity ITI estimations like the method II. However, the performances of the iterated Viterbi detection methods without guard bands are quite close but the method II gains about 0.1~0.2 dB over the method I at BER 10^{-5}.

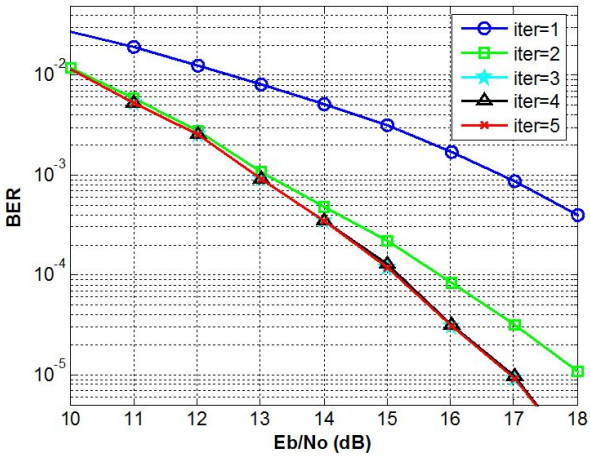

Figure 5. Performance of the iterated Viterbi method I over the number of iteration for the channel $\mathbf{H}_A$.

In Figure 6, we also compared the performance of the proposed methods with other Viterbi-based detectors i.e., the optimal 2-D Viterbi detector, which is labelled as Viterbi(64) from Burkhard (1989) and the modified Viterbi detector from Nabavi *et al.* (2007) with more parallel branches by incorporating more ITI in the trellis, labelled as Viterbi15B. The proposed methods achieve the gains of about 2 dB and 3 dB over the Viterbi(64) and Viterbi15B at BER = 10^{-5}, respectively. The proposed methods outperform over the two Viterbi-based detectors because the proposed methods yield more reliable ITI estimations between the tracks from the multi-track processing.

The performance comparison of the proposed methods and other Viterbi detectors for the BPM channel $\mathbf{H}_B$ is shown in Figure 7. For the channel $\mathbf{H}_B$, the performance gain of the proposed method II over the method I is more significant than their performance in the channel $\mathbf{H}_A$ with the gain of about 0.4 dB at BER 10^{-5}. The proposed method I without the guard bands is 2.5 dB beyond the method with the guard bands. Similar to the channel $\mathbf{H}_A$, the performances of proposed method I and II are superior to the performance of the non-iterated Viterbi detectors.

Moreover, we also investigated the performance of the proposed methods for the BPM channels in the presence of media noise due to the size and location fluctuation of bit islands with the standard deviation of fluctuation as the percentage of the bit period. Here, a higher areal density of 2 Tb/in^2 is considered. We generate the perpendicular BPM channel response using the 2-D Gaussian function with media noise from Equation 4. For the areal density of 2 Tb/in^2, we select the bit period T_x and the track pitch T_z to be 18 nm and the 2-D Gaussian pulse response has an along-track PW50 of 19.4 nm and a cross-track PW50 of 24.8 nm, for a square island with length 11 nm and thickness 10 nm and a magneto-resistance (MR) read-head with the specific parameters from Nabavi *et al*. (2009). The 3x3 channel response matrix without media noise generated using the 2-D Gaussian function is

$$\mathbf{H}_{Gau} = \begin{pmatrix} 0.0213 & 0.2321 & 0.0213 \\ 0.0919 & 1 & 0.0919 \\ 0.0213 & 0.2321 & 0.0213 \end{pmatrix}. \quad (16)$$

Even though the areal density is increased to 2 Tb/in^2 by reducing the periods in both directions in the new channel, the values of the ISI and ITI coefficients in the new channel matrix are similar to those in the previous channel at 1 Tb/in^2 density because the size of island in here is also smaller than the previous channel. However, the higher density and smaller island size will suffer more media noise. We consider the fluctuation of location and size with standard deviation 3%, 6%, and 9% of the pit period. The location and size fluctuation will increase the level of interference in the channel. For example, the random media noise level of 6% gives a channel matrix

$$\mathbf{H}_{Media} = \begin{pmatrix} 0.0273 & 0.3719 & 0.0222 \\ 0.0885 & 0.9985 & 0.0941 \\ 0.0204 & 0.3009 & 0.0318 \end{pmatrix}. \quad (17)$$

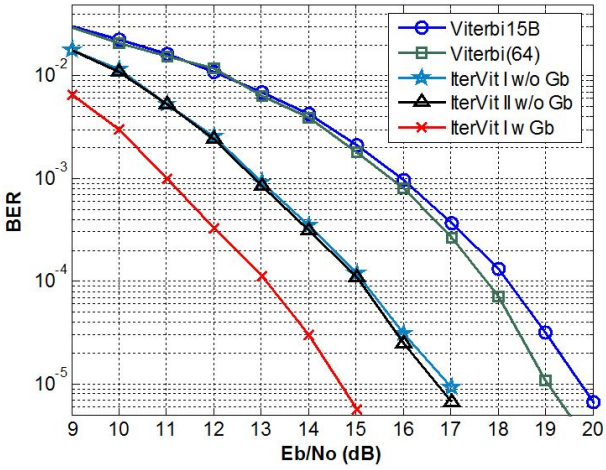

Figure 6. Performance comparison of the proposed methods with the 2-D Viterbi detectors for the channel $\mathbf{H}_A$.

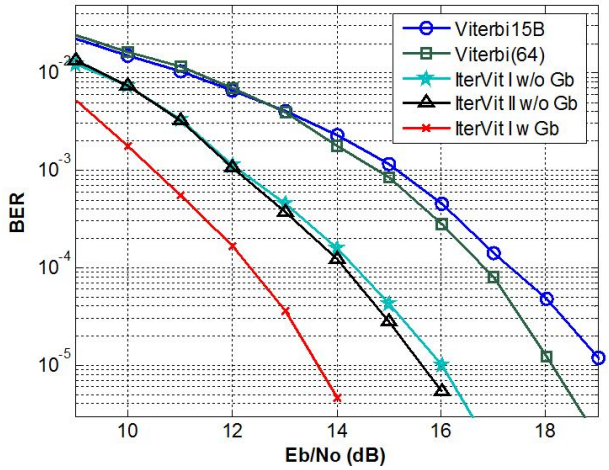

Figure 7. Performance comparison of the proposed methods with the 2-D Viterbi detectors for the channel $\mathbf{H}_B$.

Notice that the ITI level at the bits directly above and below the center bit island is increased compared with those in Equation 16.

In the simulation, we designed the trellises for the detectors using the value of coefficients from the channel response matrix without media noise first. The performance comparison of the proposed iterated Viterbi detection methods for the BPM channels with fluctuation media noise for the different values of standard deviation is shown in Figure 8. Solid lines are for the proposed method I and dashed lines are for the proposed method II. At the low value of fluctuation, the performances of the two proposed methods are similar. Whereas the fluctuation of size and location is higher, the performance difference between the two proposed methods is getting more significant. For 6% fluctuation of media noise, the proposed method II achieve about 0.5 dB gain over the proposed method I at 1x10^{-5}.

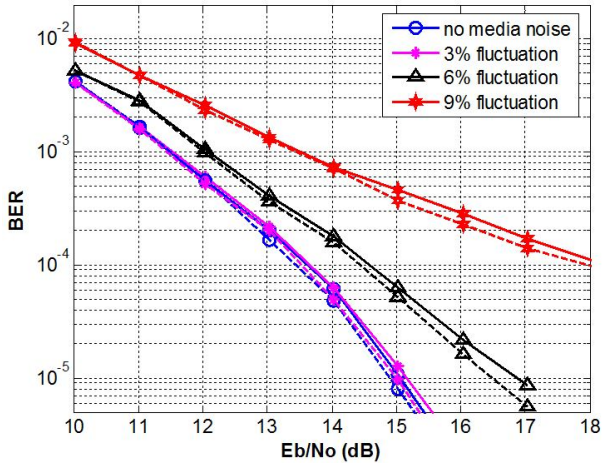

Figure 8. Performance comparison of various detectors for the BPM channels with fluctuation media noise for different values of standard deviation. Solid lines are for the proposed method I and dashed lines are for the proposed method II.

Finally, we compared the computational complexity of all detectors in this study. For the conventional Viterbi detector, the complexity, normally related to the number of total branches of its trellis, grows exponentially with the number of ISI taps in the channel. If the length of the channel is L_N, the trellis structure can have $M_s = 2^{LN-1}$ states and $B = 2$ entering or leaving branches per state node. Therefore, the total branches in the trellis can be calculated by $B.M_s$. For example, if the channel length is 3, the total number of branches in the trellis is equal $B.\ M_s = 2.2^2 = 8$. During the Viterbi algorithm, the trellis represents the state transition for estimating one input bit, in which all branches need to compute the branch metrics and all states need to update the path metric. For the branch metric calculation at each branch, one addition and one multiplication are needed as in Equation 6 and then at each state, one addition and one comparison more are required to update the path metric. Therefore, for each estimated bit, the total number of $2.B.M_s$ additions, $B.M_s$ multiplications, $B.M_s$ comparisons are required. Moreover, a lookup table with memory of $B.M_s$ is used for the branch noiseless channel outputs.

For the 2-D channel, both ISI and ITI need to be considered in the trellis structure; thus, the complexity of trellis may lead to infeasible level even with the moderate number of ISI and ITI taps. The number of states and branches in the trellis will grow exponentially with the multiplication of the number ISI and ITI taps. For the Viterbi(64) detector and the 3x3 channel matrix in this study, the number of states M_s in the trellis is $(2^3)^2 = 64$ and the number of branches per each state B is 2^3=8. In the Viterbi15B detector, the number of states M_s is equal 4, but there are 15 parallel branches between each connected paired states and each state has two groups of parallel branches. Therefore, the branch metric needs to be calculated for 2.15.4 = 120 total branches. Only a branch with the smallest branch metric from each parallel branches group is used to update the path metric, thus, the number of updating operation per bit is equal to $B.M_s = 8$. For each bit, there are 120 additions, 120 multiplications and 120 comparisons for computing the branch metric and 8 additions and 8 comparisons for updating the path metric.

In the proposed methods, the detector uses the iteration process so that the number of iterations requires to be taken into account for considering the computational complexity. In this study, the number of iteration is 3 for all detectors, thus, the number of all operations per bit is multiplied by 3 for each detector. Each method employs three detectors for three adjacent tracks but the total data block size from the three tracks is the same as the block size from the two detectors. It is not easy to compare the complexity of the two methods since the method II uses two types of detectors. However, we considered the complexity of each detector. We labeled the detectors in the method I and the detector for the middle track in the method II as an iterated Viterbi detector and a detector for the outer tracks in the method II as an iterated modified Viterbi detector. The first detector uses a very simple trellis with 4 states and two entering or outgoing branches at each state. In the iterated Viterbi detector, the trellis has two parallel branches and the complexity can be calculated similar to the Viterbi15B detector. To compare the computational complexity, the operation per data bit for each detectors is considered and compared in Table 1.

Table 1. Comparison of the computational complexity. The number of branches per data bit and the number of operation per data bit where B is the number entering branches at each state and M_s is the number of states in the trellis.

Detector name	No. of Branches	Addition	Multiplication	Comparison
Conventional Viterbi	$B.M_s$	$2.B.M_s$	$B.M_s$	$B.M_s$
Viterbi64	512	1024	512	512
Viterbi15B	120	128	120	128
Iterated Viterbi	8	48	24	24
Iterated modified Viterbi	16	72	48	48

5. Conclusions

In this paper, we apply the two iterated Viterbi detection methods for a 2-D interference BPM channel using multi-track multi-head processing. Each of the three Viterbi detectors processes a data track separately. The proposed method I applies the same trellis for all detectors but the proposed method II applies the modified trellis structures for the outer detectors to solve the problem of partial ITI estimation in the method I. The method II shows some performance gains over the method I. Even though their performances are still not as good as that of the proposed method I with the guard bands, both proposed methods achieve the significant performance gains over non-iterated 2-D Viterbi detectors due to the available ITI estimates in the iterated process.

Acknowledgements

This work is financially supported by the National Electronics and Computer Technology Center (NECTEC), the National Science and Technology Development Agency and Industry/University Cooperative Research Centre (I/U CRC) in HDD Components, and the Faculty of Engineering, Khon Kaen University, Thailand under grant no. CPN-R&D 01-20-52 EF.

References

Burkhadt, H. 1989. Optimal data retrieval for high density storage. Proceedings of the Institute of Electrical and Electronics Engineers Conference on VLSI and Microelectronic Applications in Intelligent Peripherals and their Interconnection Networks (CompEuro 89), Hamburg, Germany, May 8-12, 1989, 43-48.

Heanue, J.K., Gurkan, K. and Hessenlink, L. 1996. Signal detection for page-access optical memories with intersymbol interference. Journal of Applied Optics. 35, 14, 2431-2438.

Hekstra, A., Coene, W. and Immink, A. 2007. Refinements of multi-track Viterbi bit-detection. The Institute of Electrical and Electronics Engineers Transactions on Magnetics. 43, 7, 3333-3339.

Karakulak, S., Seigel, P.H., Wolf, J.K. and Bertram, H.N. 2008a. A new read channel model for patterned media storage. The Institute of Electrical and Electronics Engineers Transactions on Magnetics. 44, 1, 193-197.

Karakulak, S., Seigel, P.H., Wolf, J.K. and Bertram, H.N. 2008b. Equalization and detection for patterned media recording. Digests of the Institute of Electrical and Electronics Engineers International Magnetic Conference 2008, Madrid, Spain, May 4-8, 2008, HT10.

Keskinoz, M. 2008. Two-dimensional equalization detection for patterned media storage. The Institute of Electrical and Electronics Engineers Transactions on Magnetics. 44, 4, 533-539.

Nabavi, S. and Kumar, B.V.K.V. 2007. Two-dimensional generalized partial response equalizer for bit patterned media. Proceedings of the Institute of Electrical and Electronics Engineers International Conference on Communications 2007, Glasgow, Scotland, June 24-28, 2007, 6249-6254.

Nabavi, S., Kumar, B.V.K.V. and Zhu, J.G. 2007. Modifying Viterbi algorithm to mitigate intertrack interference in bit-patterned media. The Institute of Electrical and Electronics Engineers Transactions on Magnetics. 43, 6, 2274-2276.

Nabavi, S., Kumar, B.V.K.V. and Bain, J.A. 2008, Two-dimensional pulse response and media noise modeling for bit-patterned media. The Institute of Electrical and Electronics Engineers Transactions on Magnetics. 44, 11, 3789-3792.

Nabavi, S., Kumar, B.V.K.V., Bain, J.A., Hogg, C. and Majetich, S. A. 2009. Application of image processing to characterize patterning noise in self-assembled nano-masks for bit-patterned media. The Institute of Electrical and Electronics Engineers Transactions on Magnetics. 45, 10, 3523-3527.

Nutter, P.W., Ntokas, I.T. and Middleton, B.K. 2005. An investigation of the effects of media characteristics on read channel performance for patterned media storage. The Institute of Electrical and Electronics Engineers Transactions on Magnetics. 41, 11, 4327-4334.

Shiroishi, Y., Fukuda, K, Tagawa, I., Iwasaki, H., Takenoiri, S., Tanaka, H., Mutoh, H. and Yoshikawa, N. 2009. Future option for HDD storage. The Institute of Electrical and Electronics Engineers Transactions on Magnetics, 45, 10, 3816-3822.

Vucetic, B. and Yuan, J. 2000. Turbo codes: principles and applications. Kluwer Academic Publisher, Massachusetts, U.S.A. pp. 124.